The Influence of Surface Enhancement by Low Plasticity Burnishing on the Corrosion Fatigue Performance of AA7075-T6

Paul S. Prevéy (pprevey@lambda-research.com)
Lambda Research, 5521 Fair Lane, Cincinnati, Ohio 45227

John T. Cammett (cammettjt@navair.navy.mil)
Naval Aviation Depot, PSC Box 8021, MCAS Cherry Point, NC 28533

ABSTRACT

Conventional approaches to mitigate corrosion related failure mechanisms in aircraft usually involve isolation from the corrosive environment via protective coatings, alloy substitution, or modifications in design to reduce stresses. This paper describes an alternate approach employing surface enhancement by low plasticity burnishing (LPB) to eliminate or reduce the surface tensile stresses necessary for corrosion fatigue failure in AA7075-T6, without alteration of environment, material or component design.

The restoration of fatigue performance by LPB processing of AA7075-T6 after severe pitting in salt fog was previously described.[1] This paper describes benefits of introducing a deep compressive residual stress by LPB on fatigue strength after salt fog pitting and corrosion fatigue (under active corrosion) performance. Since LPB processing was performed in a conventional CNC machining center, it offers a cost effective and practical alternative to alloy substitution or component re-design as a means of improving the structural integrity of aging aircraft.

KEY WORDS: Fatigue, stress corrosion cracking, aging aircraft, corrosion, surface enhancement, and low plasticity burnishing.

INTRODUCTION

The pronounced fatigue strength reduction caused by salt pit corrosion or corrosion fatigue in a marine environment is well established for both steels[2,3] and aluminum alloys.[4] The fatigue strength debit for either mechanism is typically on the order of half the long-life, high cycle fatigue endurance limit. Corrosion pits are a common site of fatigue crack initiation in the aluminum alloy 7075-T6 widely used for structural components of older aircraft. Pitting arises from intergranular corrosion to a depth dependent upon the service environment and the time of exposure, i.e., age of the aircraft. Current annual costs for corrosion inspection and repair of military aircraft alone are estimated to exceed one billion dollars. Currently, more than 30% of military aircraft are over 20 years old and over 90% are expected to exceed a 20-year life by the year 2015.[5] The total cost of ownership and fleet readiness are adversely affected. A means of mitigating corrosion and corrosion-related fatigue damage is needed.

Low plasticity burnishing (LPB)[6,10] can provide a layer of compressive residual stress of sufficient depth to effectively eliminate the fatigue debit from prior salt pit corrosion.[1] The LPB process can be performed on conventional CNC machine tools in a shop environment at speeds comparable to machining operations. The residual stress distributions developed by LPB in nickel[6], titanium,[7] and aluminum alloys and steels[1, 3] can exceed 1 mm in depth, well beyond the depth of typical corrosion pits, which serve as the initiation sites for fatigue cracks.

LPB applied *after* salt fog corrosion pitting of AA7075-T6 has been shown to fully restore the HCF fatigue strength, eliminating the corrosion debit.[1] The initial study was designed to

investigate whether removal of the corrosion damaged layer could be avoided during overhaul. The current investigation addresses the effect of LPB processing *prior* to pitting corrosion or corrosion fatigue simulating either original manufacture or repair in which the corroded layer is removed.

EXPERIMENTAL TECHNIQUE

Material

Aluminum alloy 7075-T6 was acquired in the form of ½ inch plate to AMS 4045. The material was found to have a hardness of 89 HR.B and electrical conductivity of 33.0% IACS in accord with acceptable properties per AMS 2658. Chemistry was verified to be within the limits of the AMS 4045 specification, as shown in Table 1. Tensile properties were verified as UTS = 601 MPa (87.3 ksi), 0.2% yield strength = 542 MPa (78.7 ksi) with uniform elongation of 11%.

TABLE I
7075-T6 ½ in. Plate Composition

Element	Plate Analysis (Wt %)	AMS 4045 Limits
Zn	5.5	5.1-6.1
Mg	2.44	2.1-2.9
Cu	1.45	1.2-2.0
Fe	0.25	0.7 max
Cr	0.19	0.18-0.40
Si	0.07	0.50 max
Ti	--	0.20 max
Mn	--	0.30 max
Al	Remainder	Remainder

Low Plasticity Burnishing

Low plasticity burnishing (LPB) produces a layer of compressive residual stress of high magnitude and depth with minimal cold work.[8] The process has been described in detail previously.[1,9] It is usually performed using a single pass of a smooth free rolling ball under a normal force sufficient to plastically deform the surface of the material. Hertzian loading creates a layer of compressive residual stress to a depth exceeding 1 mm. The ball is supported in a fluid bearing with sufficient pressure to lift the ball off the surface of the retaining spherical socket. The ball is in solid contact only with the surface to be burnished and is free to roll on the surface of the work piece. Using CNC positioning, the tool path is controlled so that the surface is covered with a series of passes at a separation maintained to achieve maximum compression with minimum cold working. The tool may be moved in any direction along the surface of a complex work piece, as in a typical multi-axis CNC machining operation.

X-ray Diffraction Surface Characterization

Diffraction peak broadening, measured along with the residual stress, allows the amount of damage developed by surface enhancement methods to be accurately assessed. The method of quantifying the degree of cold working of metals, by relating the x-ray diffraction peak broadening to the equivalent true plastic strain, has been described previously.[10] The distribution of cold work as a function of depth into the deformed surface can be expressed in terms of the equivalent true plastic strain. If the degree of cold work is taken to be the equivalent amount of true plastic strain, the degree of cold work is then cumulative and is independent of the mode of deformation. Thus, the yield strength–depth distribution can then be estimated from true stress-strain curves.[10] The macroscopic residual stress-depth distribution, of primary interest in design and life prediction, was determined in the conventional manner from the shift in the diffraction peak position.[11,12,13]

High Cycle Fatigue (HCF) Testing

Four-point bending was the HCF testing mode selected to provide maximum sensitivity to the surface condition.[14] Testing was conducted at room temperature under constant sinusoidal load amplitude at 30 Hz and stress ratio, R=0.1. Active corrosion fatigue tests were conducted with the sample gage section wrapped in chemical-free laboratory tissues saturated with 3.5-wt% NaCl solution and sealed by wrapping in polyethylene film to avoid evaporation. The corroding solution was applied only at the start of the fatigue test and contacted the sample surface for the duration of the test while the sample was under cyclic loading.

Fatigue specimens had a trapezoidal cross section designed especially for the testing of highly

compressive surface conditions created by surface enhancement methods.[15] This specimen design provided a nominally 12.7 mm (0.5 in.) wide by 25.4 mm (1-in.) long region under uniform applied stress to minimize scatter in fatigue testing. The original gage section thickness of nominally 9.4 mm (0.375 in.) was chosen to be adequate to support the tensile stresses induced in the back of the specimen when a deep, highly compressive layer was formed on the test surface. The gage section thickness was then reduced to 6.2 mm (0.25 in.) by milling the backside to insure failure out of the highly compressive surface in four-point bending. The specimens were finish machined by conventional end milling to simulate the surface conditions, including residual stress and cold work, that would be present on a machined structural aircraft component manufactured from 7075-T6. Fatigue data were developed as S/N curves of nominally eight samples each for the following combinations of surface condition, corrosion damage, or corrosive environment:

1. Machined baseline
2. Machined + 100 hr. salt fog
3. Machined + active corner fatigue
4. Machined + LPB + 100hr. salt fog exposure
5. Machined + LPB + active corrosion fatigue

Detailed fractography was performed on selected specimens using both optical microscopy using a Zeiss Universal optical microscope and a Scanning Electron Microscope, Cambridge S90B SEM.

Salt Fog Corrosion Exposure

The salt fog exposures were performed at 35° C per ASTM B117 for a period of 100 hours. The fog produced was such that 1.0-2.0 ml/hr. of NaCl aqueous solution collected on each 80 cm^2 of horizontal surface. The pH of the solution was maintained between 6.5 and 7.2. Following exposure to the salt fog, the samples were soaked and then rinsed in tap water, followed with a distilled water rinse to remove any salt solution remaining, and then dried. Patches of gray and white corrosion product evident on the surface in Figure 1 of the samples were identified by x-ray diffraction as α- Al_2O_3. The corrosion product was not removed prior to fatigue testing.

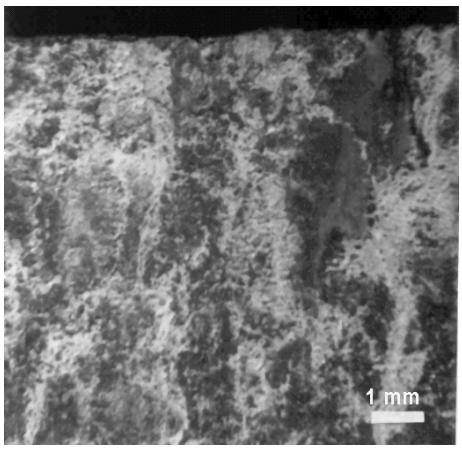

Figure 1 - Macroscopic appearance of a 7075-T6 specimen after 100-hr. salt fog exposure showing patches of Al_2O_3 corrosion product.

RESULTS AND DISCUSSION

Residual Stress Distributions

The residual stress distributions developed by machining and LPB processing are shown in Figure 2. Machining produced low tension on the surface and compression of less than –68 MPa (–10 ksi) below the surface. In contrast, LPB produced maximum compression on the order of –480 MPa (–70 ksi) between the surface and a depth of nominally 0.2 mm (0.008 in.). Maximum cold work of nominally 8% was observed from the surface through the region of maximum compression, and then diminished with greater depth. The compressive layer extended to over 0.75 mm (0.030 in.), diminishing in magnitude nearly linearly with depth. X-ray diffraction measurements could not be made reliably below a depth of 0.75 mm (0.030 in.) because of the coarse grain size encountered at depths beneath the deformed surface layer.

No attempt was made to optimize the LPB parameters to achieve a specific level of residual stress or cold work that would provide the best fatigue performance. The parameters were simply chosen, based upon prior experience, to produce a deep layer of compression with available tooling. Optimizing the combination of LPB parameters (including normal force, ball

size, ball modulus, and feed) can be done to allow the residual stress and cold work distributions to be tailored to specific applications. Previous experience with LPB of IN718[6], Ti-6Al-4V[7], and 4340[3] steel indicated that by controlling the burnishing parameters, the resulting cold work and residual stress distributions can be engineered to achieve an optimal fatigue performance for a given failure mode, applied stress spectrum, and environment.

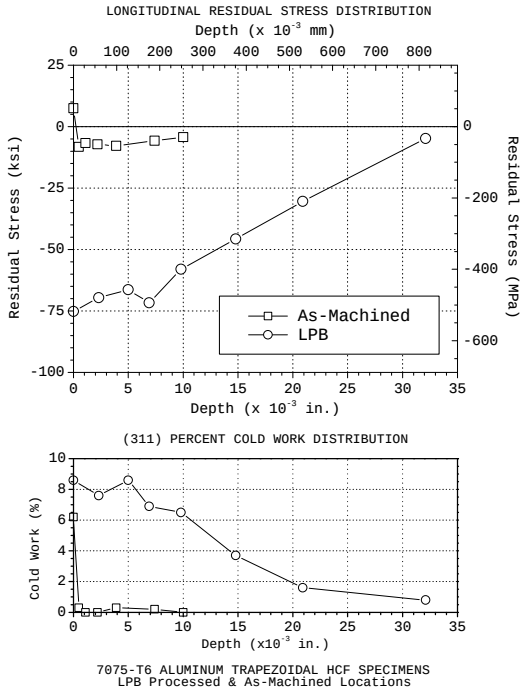

Figure 2 – Residual stress and cold work distributions produced by end milling and LPB in 7075-6.

The effect of LPB processing on the surface finish of the original machined material after 100 hr. exposure to salt fog and resulting from corrosion fatigue with prior LPB are shown in Table II. The results are the average of three repeat measurements made on each of two samples representing the conditions shown. LPB processing reduced the roughness of the original machined surface from nominally 40 to 8 μin, Ra. Salt fog exposure for 100 hr. produced a non-uniform, rough surface finish and a wide spread in surface roughness, as indicated by the high standard deviations for the corroded specimens. Active corrosion fatigue, with 3.5% NaCl solution in contact with the specimen surface for the duration of the fatigue test, produced no significant change in the initial surface roughness of either the machined or LPB surfaces.

Table II
Surface Finish of Machined and
LPB Processed 7075-T6 Aluminum

	Surface Roughness (μin, Ra)		
Surface Condition	Baseline	Corrosion Fatiuge	100h Pitting
Machined	39 ± 7	36 ± 2	139 ± 34
LPB	8 ± 3	11 ± 3	31 ± 33

Corrosion Damage

Corrosion during fatigue testing was termed "active corrosion" for the purposes of this study, to indicate that the corrosion process was active only during cyclic loading, resulting in a condition of "corrosion fatigue." In contrast, salt fog exposure prior to fatigue testing produced pitting damage, but the corrosion process was not active during fatigue loading. Fatigue testing then measured the effect of the prior damage. In this case, fatigue crack initiation from the corrosion pits is assumed not to be assisted by continuing corrosion. However, testing was conducted in ambient laboratory air at nominally 40 to 50% humidity, so the possibility of some further corrosion during testing cannot be completely ruled out.

Corrosion damage was documented both in terms of the nature of the oxide layer formed and the depth of pits. Surface oxidation was examined by optical microscopy with both low and high magnifications. Pit depths and distributions were measured at high magnification using the calibrated fine focusing adjustment on a Zeiss Universal optical microscope after removal of the surface layer of oxide corrosion product with nitric acid. Macroscopic and fractographic examination of the exposed surfaces revealed that 100-hr. salt fog exposure of the machined surface resulted in pitting corrosion distributed uniformly over the test surfaces. Typical pit depths were 100 μm to 120 μm (0.004 to 0.005 in.). After penetration of the surface, the corrosion crevices often were observed to progress laterally, thereby

delaminating layers of material and apparently following the elongated grain boundaries produced during rolling of the plate. Salt fog exposure for 100 hr. after LPB produced a different pattern of oxidation. Predominantly, circular patterns were observed in the surface oxide at higher magnification, as shown in Figure 3. Striking spiral patterns were observed at the edges of the exposed surface, as shown in Figure 4. Shallower pitting was observed on the surfaces that received LPB after machining and prior to salt fog exposure than those machined surfaces directly exposed without LPB. Pits in the LPB surfaces after 100-hr. salt fog exposure had irregular boundaries, but overall equiaxed shapes with a 34 μm (0.0014 in.) average depth and a nominal 44 μm (0.0018 in.) diameter. This is nominally one-third the depth of pitting observed for the machined samples exposed without LPB treatment.

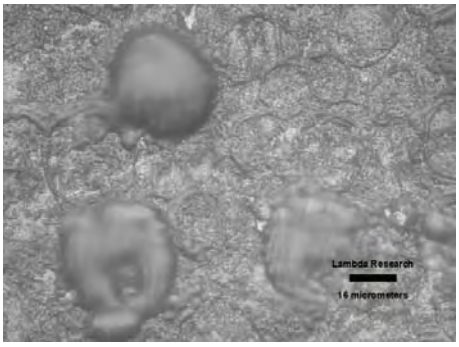

Figure 3 – Circular oxidation patterns at mid-width of an LPB 7075-T6 surface after 100 hr. salt fog exposure.

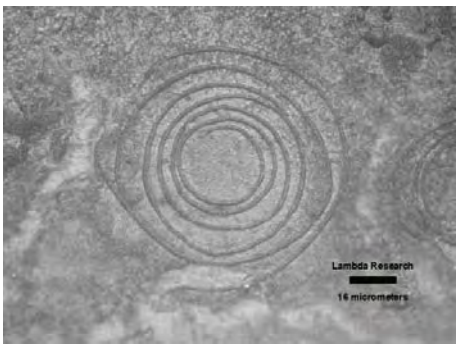

Figure 4 – Spiral oxidation patterns at the edge of an LPB 7075-T6 surface after 100 hr. salt fog exposure.

Active corrosion during fatigue cycling at ambient temperature produced much shallower pits than 100 hr. salt fog exposure at 35C, even in samples receiving the maximum exposure for the full 10^7 cycles to run-out (108 hours of testing in 3.5% NaCl solution). For both the machined and LPB surfaces, the pits were nominally 9 μm (0.0004 in.) deep and were numerous across the entire exposed surface. Pits on the machined surface tended to be circular with a nominal diameter of 5 μm (0.0002 in.). Pits on the LPB surface tended to be irregular and interconnecting, extending up to 20 μm (0.0008 in.). A typical group of pits produced by active corrosion on the machined surface is shown in Figure 5 adjacent to a region of oxide film. A comparable region in the gage section of an LPB sample is shown in Figure 6.

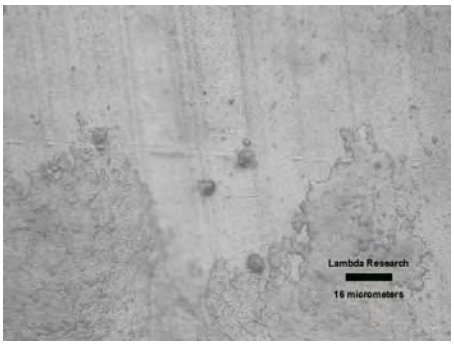

Figure 5 – Central gage section pitting and surface oxidation produced by active corrosion during fatigue testing of a machined 7075-T6 surface.

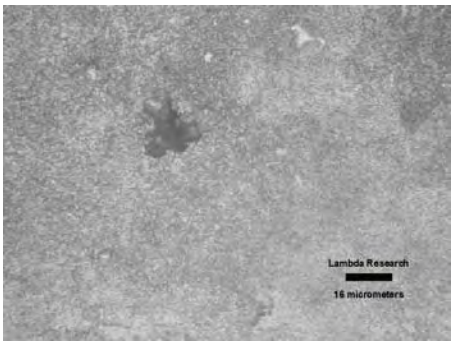

Figure 6 – Pitting and surface oxidation produced by active corrosion during fatigue testing of a 7075-T6 machined surface after LPB.

Corrosion Fatigue Performance

The S/N curves generated for 7075-T6 in both the baseline as-machined condition and with LPB after 100-hr. salt fog exposure or prior to active corrosion fatigue are presented in Figure 7. Fatigue tests were continued for a minimum of 2.5 x 10^6 cycles if no failure occurred first. Maximum run-out sustained was 1.2 x 10^7cycles.

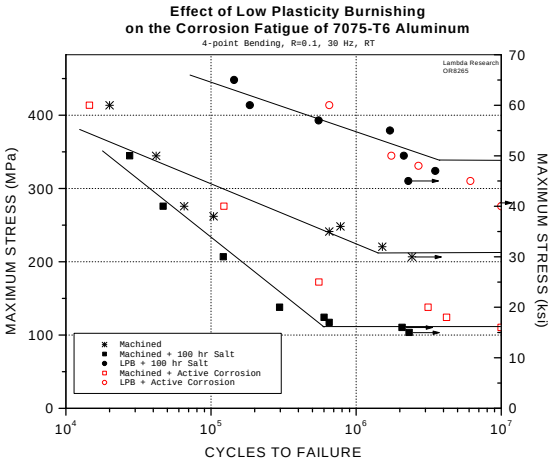

Figure 7 - High cycle fatigue results for salt fog pitted and active corrosion fatigue of machined 7075-T6 with and without LPB processing prior to exposure to corrosion.

The S-N curves for samples with pitting from prior salt fog exposure appeared to exhibit an endurance limit, implying infinite life below that stress level. The S-N curves for samples exposed to active corrosion fatigue during testing do not appear to have an endurance limit, as is commonly reported in studies of corrosion fatigue.[16] Because fatigue tests were limited in both number of samples and applied load cycles to nominally 1.0 x 10^7cycles, the presence of a true endurance limit cannot be confirmed without additional testing. In the discussion that follows, the results are considered and compared in terms of the fatigue life at nominally 2 x 10^6 cycles. The fatigue data in Figure 7 are presented as semi-logarithmic S-N curves at stress ratio, R, of 0.1, in terms of the maximum stress.

The machined (end milled) surface condition produced an apparent endurance limit on the order of 200 MPa (30 ksi). Salt fog exposure for 100 hrs. reduced the endurance limit to nominally 100 MPa (15 ksi), half that of the original machined surface before exposure to salt fog. The fractional loss of fatigue life at stress levels above the endurance limit for salt fog exposed samples increased rapidly with decreasing maximum stress level, reaching an order of magnitude at the 200 MPa (30ksi) endurance limit. Active corrosion fatigue in 3.5% NaCl solution, with no prior corrosion damage, degraded the fatigue strength relative to the as-machined condition by an amount only slightly less than for prior pitting corrosion from 100 hr. salt fog exposure up to a life of 10^7 cycles. A failure occurred in active corrosion fatigue at 10^7 cycles, i.e., at the nominal 100 MPa endurance limit for pitting corrosion. The data appear to suggest both further reduction in fatigue strength with increasing life and the absence of an endurance limit for active corrosion fatigue. LPB prior to salt fog pitting resulted in a 70% increase in the endurance limit, from nominally 200 MPa (30 ksi) to over 330 MPa (48 ksi). The fatigue life at stress levels above the 310 MPa (45 ksi) endurance limit for LPB prior to corrosion is two orders of magnitude (100X) greater than that of the baseline machined surface. A comparable benefit in fatigue performance was observed for LPB prior to active corrosion fatigue in 3.5% NaCl solution. As noted earlier, a true endurance limit may not exist for the active corrosion fatigue mechanism, however, the fatigue strength at 10^7cycles was at least 282 MPa (41ksi). Fatigue lives were 100 times that of the baseline machined surface for stress levels above 275 MPa (40 ksi).

Fractographic analysis revealed that all fatigue failures in specimens without prior LPB, whether exposed to salt fog pitting or active corrosion fatigue, initiated at the surface. A typical surface fatigue initiation site is shown in Figure 8. All salt fog pitted sample initiations were exclusively from corrosion pits, as shown in Figure 9. Specimens tested at lower stresses generally exhibited fatigue origins from a single pit, while specimens tested at higher stress levels tended to have multiple origins.

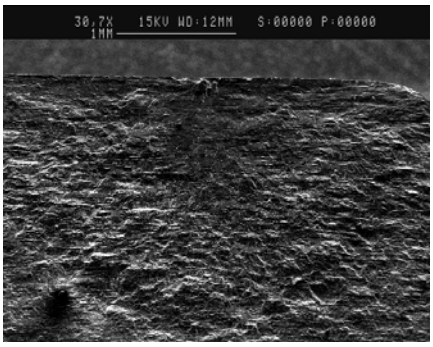

Figure 8 – Typical surface fatigue initiation site on machined 7075-T6 in active corrosion fatigue.

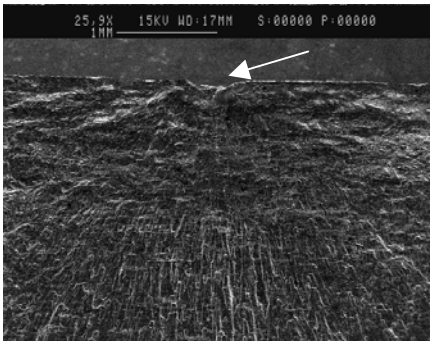

Figure 9 – Fatigue fracture surface of typical machined + 100hr salt fog exposure sample. Arrow indicates fatigue origin at the site of corrosion pit.

The effect of the layer of high residual compression produced by LPB was to drive fatigue origins below the surface by as much as 1 mm (0.04 to 0.05 in.). All fatigue cracks in the LPB + salt fog pitted samples initiated not at the damaged surface, but subsurface. The subsurface stress in bending simply exceeded the fatigue limit of the material below the compressive layer. A typical subsurface origin is shown in Figure 10. Only one active corrosion fatigue sample failed from the LPB surface. This was at the highest load tested. Subsurface initiation was observed in a previous study of LPB after pitting corrosion damage.[1] As fatigue failures did not originate at the LPB processed surface, the results can be interpreted as demonstrating that the LPB surface has even higher fatigue strength than indicated in this testing.

The subsurface initiations are thought to be associated with the tensile residual stress developed below the compressive layer. The coarse grain size of the material used in this investigation prohibited direct measurement of the maximum subsurface tensile stress. Finite element analysis and fatigue life modeling are being employed to more thoroughly analyze the subsurface failure mechanism.

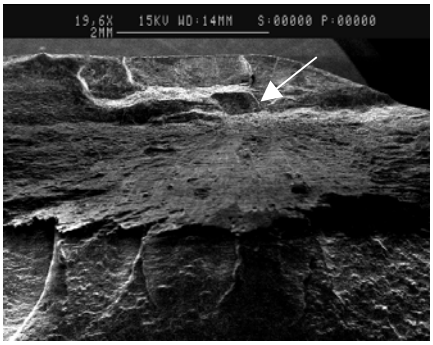

Figure 10 – Subsurface fatigue origin below the compressive layer produced by LPB.

CONCLUSIONS

The fatigue performance of the marine environment corrosion sensitive aluminum alloy 7075-T6 is greatly improved by low plasticity burnishing (LPB) prior to exposure to either salt fog pitting or active corrosion fatigue in 3.5% NaCl solution. Both corrosion mechanisms reduced the fatigue endurance limit of machined (end milled) 7075-T6 from nominally 205 MPa (30 ksi) to only 100 MPa (15 ksi), half of the original, fatigue strength. LPB prior to exposure to either corrosion mechanism increased the endurance limit to over 310 MPa (45 ksi), over three times the strength of a machined surface exposed to corrosion and 50% stronger than the un-corroded original machined surface. The fatigue life at maximum stress levels above the endurance limit is at least 100 times greater for LPB processed 7075-T6.

The improvement in fatigue life and strength are attributed to the introduction of a layer of residual compression with a magnitude and depth sufficient to suppress fatigue crack initiation and propagation, even in aggressive corrosive environments. The depth and magnitude of compression are sufficient to close cracks emanating from corrosion pits shallower than the layer of compression, rendering them innocuous, and altering the mode of fatigue crack

nucleation. In active corrosion fatigue, the compressive layer retards the growth of fatigue cracks, producing two orders of magnitude (100X) life increase at stresses above the endurance limit.

LPB prior to corrosion has been demonstrated to substantially improve the fatigue performance of the aluminum alloy 7075-T6 widely used in structural aircraft applications. The ease of implementation in standard CNC machining centers offers the possibility of employing LPB as an effective means of mitigating corrosion fatigue and pitting fatigue initiated failures in aircraft components without altering either material or design. Applied locally to high stress fatigue prone locations in aging aircraft, LPB could extend the service life of aircraft structural components, reduce the total cost of fleet ownership, and improve fleet readiness.

ACKNOWLEDGEMENTS

The authors gratefully acknowledge the contributions of Doug Hornbach and the staff of Lambda Research for the residual stress and fatigue data generated in this study.

REFERENCES

1 Prevéy, P., Cammett, J., “Low Cost Corrosion Damage Mitigation and Improved Fatigue Performance of Low Plasticity Burnished 7075-T6,” *JMEP*, **10(5)**, ASM Intl, Materials Park, OH, Oct. 2001, pp. 548-555.

2 ASM Handbook, Vol. 19, Fatigue and Fracture, S.R. Lampman, ed., ASM International, Metals Park, OH, 1996, pp. 596-597.

3 Cammett, J. and Prevéy, P., “Fatigue Strength Restoration in Corrosion Pitted 4340 Alloy Steel via Low Plasticity Burnishing,” (2001), Retrieved July 19, 2002, from http://www.lambda-research.com/publica.htm.

4 Dowling, N., Mechanical Behavior of Materials, Prentice Hall, NJ, 1993, p. 365.

5 Agarawala, V., "Corrosion and Aging: Aircraft Concerns," presentation at 11th Annual AeroMat Conference, Bellevue, WA, June 26-29, 2000.

6 Prevéy, P., Telesman, J., Gabb, T., Kantzos, P., "FOD Resistance and Fatigue Crack Arrest in Low Plasticity Burnished IN718," Proceedings of the 5th Nat. Turbine Eng. HCF Conference, 2000.

7 Prevéy, P. and Shepard, M., "Surface Enhancement of Ti-6Al-4V Using Low Plasticity Burnishing," Presentation at 11th AeroMat Conference, Bellevue, WA, June 2000.

8 U.S. Patent 5,826,453 (Oct. 1998), other patents pending.

9 Prevéy, P., Hornbach, D., Mason, P., “Thermal Residual Stress Relaxation and Distortion in Surface Enhanced Gas Turbine Engine Components,” Proc. ASM Materials Week, Indianapolis, IN, Sept. 15-18, 1997

10 Prevey, P., Residual Stress in Design, Process & Material Selection, ASM, Metals Park, OH, (1987) pp. 11-19.

11 Prevéy, P., Metals Handbook, Vol 10, ASM, Metals Park, OH, (1986) pp. 380-392.

12 Hilley, M., ed., Residual Stress Measurement by XRD, SAE J784a, SAE, Warrendale, PA (2001).

13 Noyan & Cohen (1987) Residual Stress Measurement by Diffraction & Interpretation, Springer-Verlag, NY.

14 Prevéy, P., Koster, W.P., (1972) “Effect of Surface Integrity on Fatigue of Standard Alloys at Elevated Temperatures,” Fatigue at Elevated Temperatures, ASTM STP561, ASTM, Phil., PA, pp. 522-531.

15 Prevéy, P., et al, “Low Cost Surface Enhancement Method for Improved Fatigue Life of Superalloys at Engine Temperature,” NAS3-99116 SBIR, NASA final report, March, 2001.

16 Frost, N.E., Marsh, K.J., and Pook, LP, Metal Fatigue, Dover, NY, 1974, pp105-112.